Proceedings of the ECCOMAS Thematic International Conference on Simulation and Modeling of Biological Flows (SIMBIO 2011)
September 21-23, 2011, VUB, Brussels, Belgium

Analysis of the fluid dynamic characteristics of the obstructive pulmonary diseases using a three-dimensional cfd model of the upper conductive zone of the lung airways.

Ana F. Tena[1], Pere Casan[1], Alfonso Marcos[2], Raúl Barrio[3], Eduardo Blanco[3]

1 Instituto N. de Silicosis. C/ Dr Bellmunt. 33006 Oviedo, Spain. E-mail: anafertena@gmail.com, pcasan@ins.es
3 Universidad de Oviedo. C. de Viesques 33203 Gijón, Spain. E-mail: barrioraul@uniovi.es; eblanco@uniovi.es
2 Universidad de Extremadura. Avda de Elvas, 06071 Badajoz, Spain. E-mail: acmarcos@unex.es

Abstract

The main objective of this work is the analysis of the fluid dynamic characteristics of the obstructive pulmonary diseases (Cronic Obstructive Pulmonary Disease, COPD, bronchitis and emphysema). Its obstructive pattern can be easily detected in the spirometry, but they usually need more complex tests to distinguish between them. However, their fluid dynamic features are quite different.

A 3D numerical model of the bronchial tree has been developed, from the trachea to the seventh level bronchioles, following the model developed by Weibel and Kitaoka . The main innovation in the numerical model is the unsteady boundary conditions applied and an adaptive time step, using two User Defined Function (UDF). The analysis of the results obtained varying the geometry and the unsteady boundary conditions, allows the characterization of the particular fluid dynamic phenomenon of each disease and how it is perceived in the tests.

Keywords: obstructive pulmonary disease, spirometry, CFD.

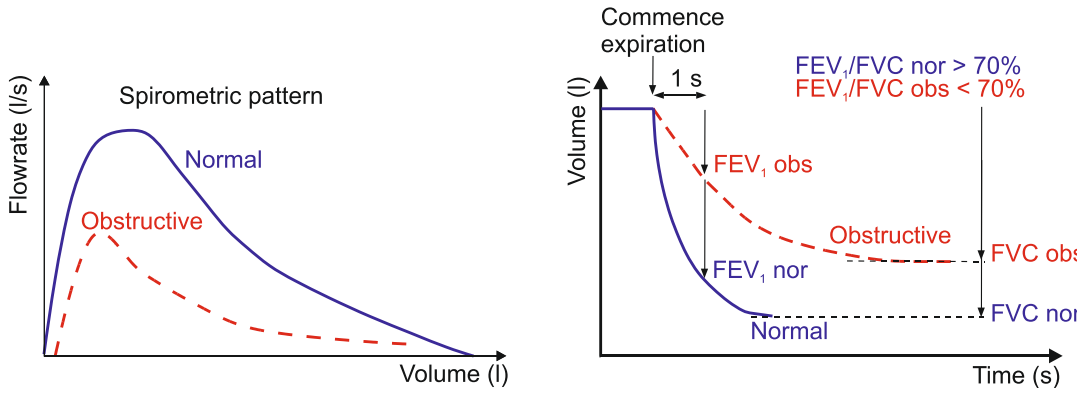

Fig.1 Normal and obstructive curves obtained in the forced spirometry test

Introduction

Lung diseases with an obstructive diagnosis are, basically, COPD (Cronic Obstructive Pulmonary Disease, both bronchitis and emphysema), and asthma although some other diseases and entities as tumors can also hinder the air flow. Its obstructive pattern can be easily detected in the spirometry (figure 1), but they usually need more complex tests to distinguish between them. However, their fluid dynamic features are quite different.

The distinctive attribute between COPD and asthma is the chronic quality of the first. A nearly normal pulmonary function can be observed in asthma patients after a bronchodilator treatment.

The main fluid dynamic effect in bronchitis is produced by the section reduction of the airways, mainly due to the chronic inflammation. The pressure loss increases and the flow rate diminish, mainly during the first second, when air velocity is the highest. As the global airways section increases going down the bronchial tree, is to be expected that the obstruction of the lower order branches is the most significant part of the phenomena. As the flow can be considered laminar, at

least in the less severe phase of the illness, the pressure loss should be more or less proportional to the flow rate. The presence of an obstruction originated by a tumor, on the other hand, can be considered as a singular pressure loss, and influenced by the square of the flow rate.

The respiratory obstruction generated by emphysema has a completely different source: the pressure driving the flow during the expiratory maneuver is due to the elastic lung recoil; in emphysema, the loss of elastic tissue elements reduces this pressure, hampering the lungs deflation [1].

A normal description of the human lung with 24 branches must have 16 million of segments (2^{24}). A full CFD resolution requires an estimated mesh size of thousands of millions of elements. CFD simulations have been limited to relatively small subsections of the lung geometry, being the flow in the lower airways either ignored or modeled using simple 1D or axisymmetric approximations. The earliest morphological description of the lung was the symmetric model of Weibel [2]. A complementary alternative was proposed by Kitaoka et al. [3]. Now, there are several models, most of them derived from these. Realistic morphologies for lung airways up to nine branches can be obtained using CT-scan and MRI techniques [4, 5].

Several works have demonstrated the complexity of the pulmonary flow. Zhang and Kleinstreuer [6] performed CFD simulations in a four-generation symmetric branching model and found that unsteady typical flow of normal breathing led to different flow features than in the steady state case, being greater during high frequency ventilation. Luo et al. [7] investigated the effect of COPD on particle deposition in the upper lung airways for a symmetric four-generation model. Yang et al. [8] worked with a three-generation airway model for both healthy and COPD cases, and found that the velocity profile entering the segments has great influence on flow patterns and pressure drop.

The main innovation in this numerical model is the unsteady boundary conditions applied [9, 10]. Volume and flow rate (vs. time) real data have been obtained from forced spirometry tests of patients without obstructive pulmonary diseases. This data has been used with the model to obtain the pressure vs. volume and pressure vs. time patterns at the end of the smaller bronchioles studied. Then, with these boundary conditions, were made simulations under obstructive pulmonary diseases (bronchitis and emphysema). The analysis of the results obtained varying the geometry and the unsteady boundary conditions, allows the characterization of the particular fluid dynamic phenomenon of each disease and how it is perceived in the tests.

Methodology and numerical model

Few forced spirometry tests of patients without obstructive pulmonary diseases were realized to simulate realistic conditions. From these data relations between volume, flow rate and time have been obtained (Fig. 2).

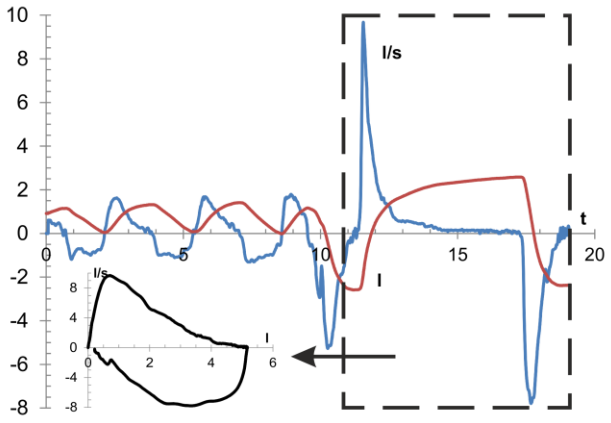

Fig.2 Forced spirometry tests.

A 3D numerical model of the bronchial tree has been developed, from the trachea to the seventh level bronchioles. The geometry follows the model developed by Weibel [2] and Kitoaka et al [3]. The dimensions of the built model can be seen in table 1.

Table 1: model dimensions

Gen	Branches	Diam (m)	Lengh (m)	Area (m^2)
0	1	0.018	0.12	0.000254469
1	2	0.012211422	0.047822285	0.000117118
2	4	0.00828438	0.019058091	5.39026E-05
3	8	0.005620225	0.007595012	2.48083E-05
4	16	0.00445127	0.012665425	1.55617E-05
5	32	0.003512926	0.010685373	9.69232E-06
6	64	0.002807205	0.009014874	6.18925E-06
7	128	0.002271429	0.007605532	4.05218E-06

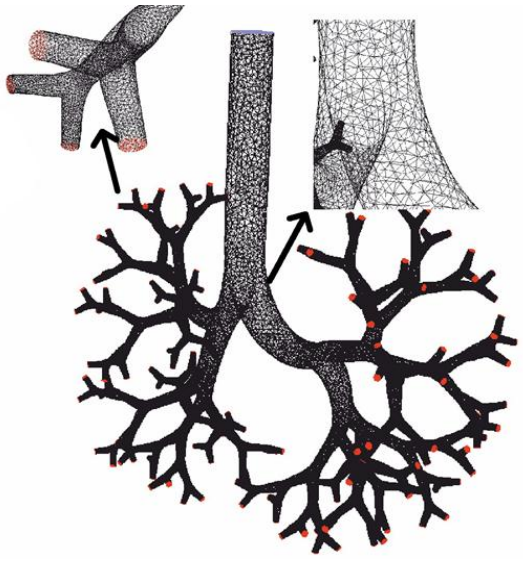

Fig.3 Numerical model and detail of the surface mesh.

Figure 3 shows a global image of the unstructured mesh generated. The total number of cells used to begin with the simulations was about 10^6, though other meshes of different size (2 10^6 and 4 10^6) were generated in order to investigate the dependence of the numerical predictions. As can be seen in Fig 4, the variation observed in the outlet flow rate when considering different mesh sizes is not very significant. For the mesh size used for the calculations (about 1,000,000 cells) this variation is lower than 1.11%, and with 2,000,000 cells is lower than 0.67% compared with the model of 4,000,000 cells.

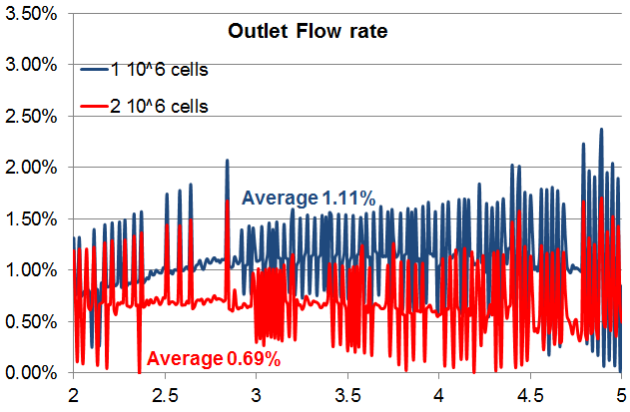

Fig.4 Results of the independence tests.

The maximum equiangle skew was restricted below 0.6 for 98% of the cells in the mesh.

The numerical simulations were performed with the code Ansys Fluent [11]. This code was used to solve the full unsteady 3D Navier-Stokes equations by the finite volume method. Air is the working fluid with a constant density of 1.225 kg/m^3 and dynamic viscosity of 1.7894 10^{-5} kg/(m s).

The boundary conditions imposed were firstly an unsteady velocity distribution (using a User Defined Function) at the inlet (G0, trachea) and gauge static pressure at the outlet (G7).

The number of time steps was 400. Due to non-uniformity of breathing cycle, it was applied an adaptive time step method by means of the before User Defined Function. The number of iterations in each time step was adjusted to reduce the magnitude of the residuals below an acceptable level. The residuals converged quickly and reached negligible magnitudes.

The time required for each simulation was 4 days working in parallel with 4 cores. Over 5 breathing cycles are necessary to achieve the periodic unsteady solution convergence.

Figure 5 shows the inlet boundary condition (unsteady flow rate) obtained from a forced spirometry test, and the unsteady pressure pick-up from the simulation.

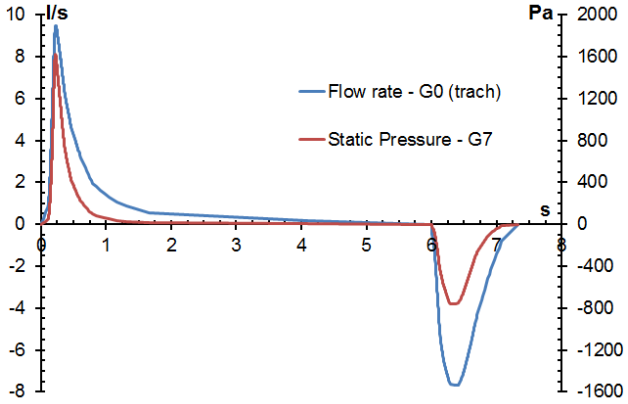

Fig.5 Unsteady flow rate imposed and static pressure obtained.

One way to check if the simulation is right is to repeat the test, but in this case the unsteady pressure obtained before as inlet boundary condition (G7) and see if it matches the obtained unsteady output velocity (G0, trachea) with the first valor (fig. 6). Results look like rights.

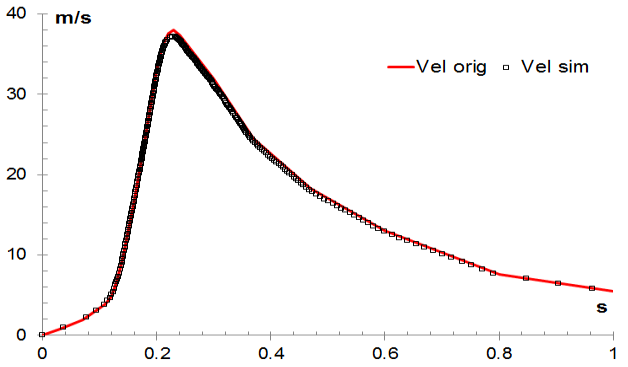

Fig.6. Real and simulated velocities in the trachea (G0)

To simulate the COPD conditions (bronchitis and emphysema) the unsteady total pressure obtained in the past step is imposed as the inlet (G7) boundary condition using an udf whereas a gauge pressure is established as the outlet boundary condition. In the case of bronchitis, the roughness of the walls was increased, whereas in the case of emphysema, a branch of order 3 was closed, which is equivalent to having 1/8 of inoperable lung.

Results

First of all, the results will be compared with those existing in the literature. Hofmann et al [12] say that the velocity is increasing in the first branches, from the branch 0 (trachea) to branch 3. Rest of the branches, from G4 to 24, the velocity is decreasing.

The total sections of the built model are in the table 2. Figure 7 shows the velocity magnitude obtained in the simulation in the different pulmonary branches for a healthy lung. From the G0 (trachea) to G3 the velocity is increasing, whereas in the rest is decreasing. Therefore, both results are in agreement.

Table 2: Variation of the total section in the airways

Gen	Total area (m^2)	Gen	Total area (m^2)
0	0.00025447	4	0.00024899
1	0.00023424	5	0.00031015
2	0.00021561	6	0.00039611
3	0.00019847	7	0.00051868

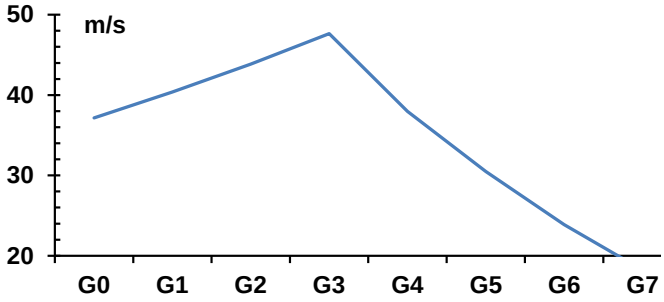

Fig.7. Velocity magnitude in the pulmonary branches

Figure 8 shows the pahtlines from G7 to the trachea (G0) colored by inlet surface, and the velocity vectors in first 3 branches at a given moment of the expiratory flow.

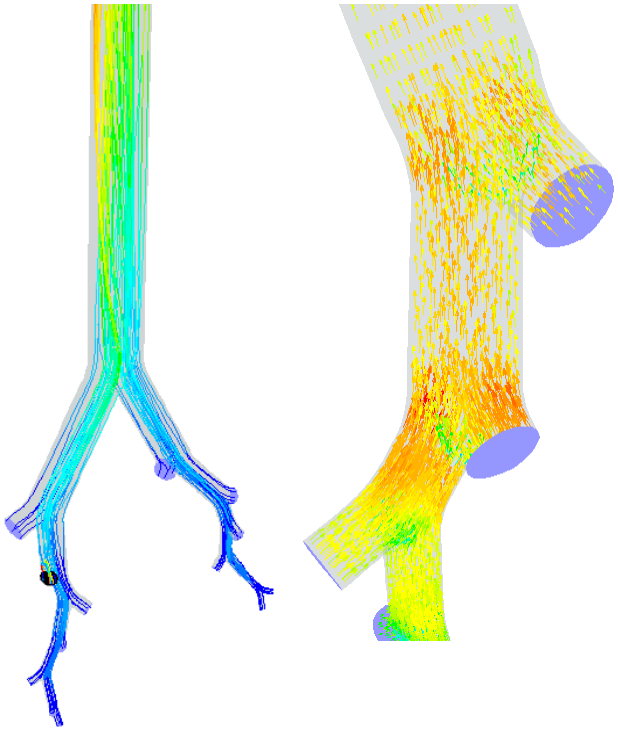

Fig.8. Pathlines from G7 to G0 in two branches and velocity vector in first 3 branches.

For the same flow conditions, Figure 9 shows the contours of velocity in cross sections of different branches, in the sense of clockwise. In general, the flow is axisymmetric, with predominant axial component of velocity.

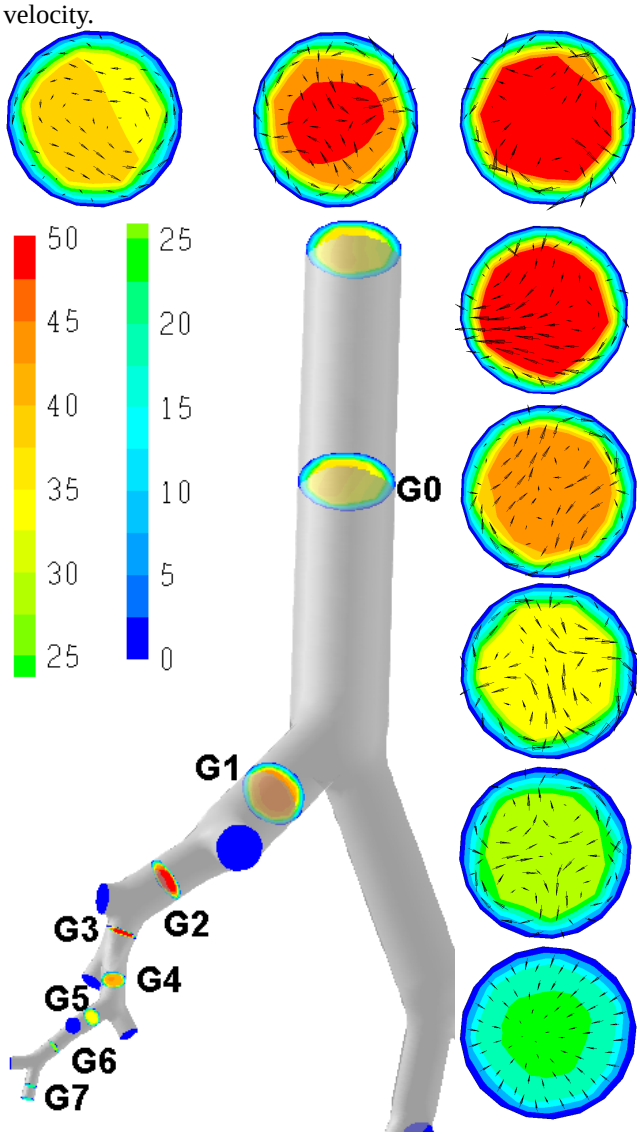

Fig.9. Contours of velocity in cross sections of different branches.

Figure 10 shows the unsteady velocity in the trachea (G0) for the three study cases, with the same inlet boundary condition (static pressure), as has been said previously. The conditions imposed to simulate bronchitis and emphysema correspond, in this first study, a mild conditions. The simulation perfectly captures these situations, with results similar to those obtained by spirometry tests. The spirometry results are shown as graphics of flow rate versus volume and volume versus time. To obtain these values, previous results are integrated, being shown in Figures 11 (flow rate vs volume) and 12 (volume vs time).

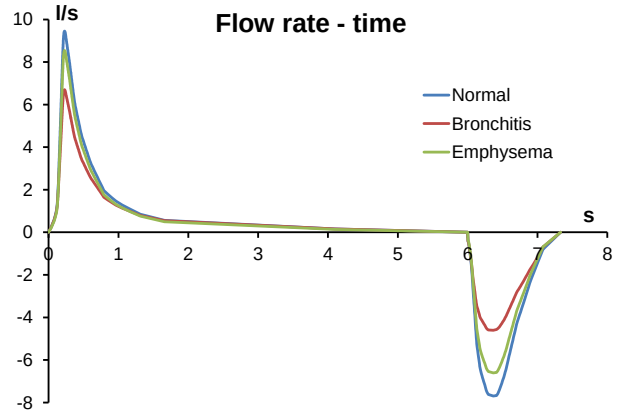

Fig.10. Velocity magnitude in the pulmonary branches

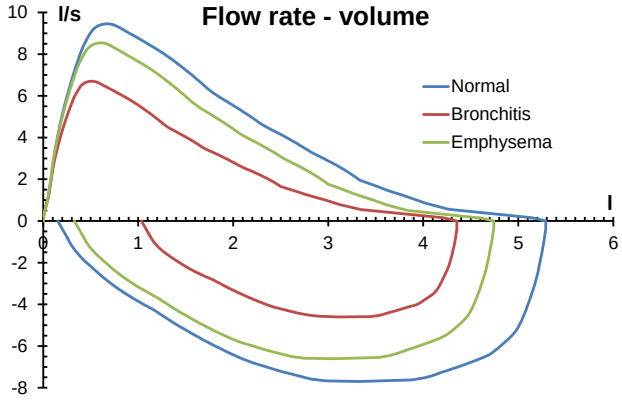

Fig.11. Flowrate versus volume.

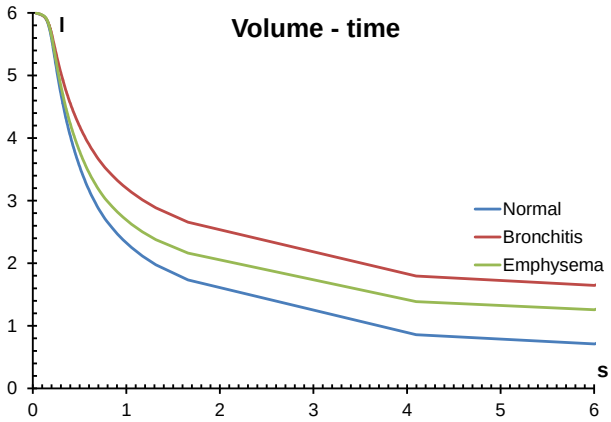

Fig.12. Volume versus time.

From these data it can be obtained the most used parameters in pneumological studies (FVC, Forced Vital Capacity; FVC_1, Forced Expiratory Volume in first second; FEF_{25-75}, Forced Expiratory Flow at 25% point to the 75% point of Forced Vital Capacity; PEF, Peak Expiratory Flow). Table 3 shows these parameters.

Table 3

	Normal	**Bronchitis**	**Emphysema**
	l	***l***	***l***
FVC	5.29	4.35	4.74
FVC_1	3.69	2.81	3.29
	l/s	***l/s***	***l/s***
PEF	9.46	6.70	8.54
	%	***%***	***%***
FVC_1/FVC	72.68%	64.56%	69.34%

Conclusions

A numerical study of lung diseases with an obstructive diagnosis (COPD) was made using unsteady boundary conditions. These boundary conditions were imposed by means of two User Defined Functions (UDF's), one to obtain the unsteady pressure in the branch G7 and the other to obtain the spirometry data in the three study cases.

Once verified the functioning of the model, further studies will be directed to simulate different cases of existing spirometry.

Acknowledgements

The authors gratefully acknowledge the financial support provided by Junta de Extremadura and FEDER under project GR10047 and also by Ministerio de Ciencia e Innovación under project DPI 2010-21103-C04-04.

References

[1] R.J. Altiere and D.C. Thompson, Physiology and Pharmacology of the Airways. In: Inhalation Aerosols, 2d Edition, Informa Healthcare (2007).

[2] E.R. Weibel, Morphometry of the human lung, Springer-Verlag (1963).

[3] Kitaoka, H., Takaki, R., and Suki, B., 1999, "A Three Dimensional Model of the Human Airway Tree" J. Appl. Physiol., 87(6), pp. 2207–2217.

[4] Sera, T., Fujioka, H., Yokota, H., Makinouchi, A., Himeno, R., Schroter, R. C., and Tanishita, K., 2003, "Three-Dimensional Visualization and Morphometry of Small Airways From Microfocal X-Ray Computed Tomography," J. Biomech., 36(11), pp. 1587–1594.

[5] Burton, R. T., Isaacs, K. K., Fleming, J. S., and Martonen, T. B., 2004, "Computer Reconstruction of a Human Lung Boundary Model From Magnetic Resonance Images," Respir. Care, 49(2), pp. 180–185.

[6] Zhang, Z., and Kleinstreuer, C., 2011, "Computational analysis of airflow and nano particle deposition in a combined nasal–oral–tracheobronchial airway model," Journal of Aerosol Science 42, pp. 174–194.

[7] Luo, H. Y., Liu, Y., and Yang, X. L., 2007, "Particle Deposition in Obstructed Airways," J. Biomech., 40(14), pp. 3096–3104.
[8] Yang, X. L., Liu, Y., So, R. M. C., and Yang, J. M., 2006, "The Effect of Inlet Velocity Profile on the Bifurcation COPD Airway Flow," Comput. Biol. Med., 36(2), pp. 181–194.
[9] R.K. Freitas and W. Schröder, 2008, Numerical investigation of the three-dimensional flow in a human lung model, Journal of Biomechanics 41, pp. 2446–2457.
[10] C-L. Lin, M.H. Tawhai, G. McLennan, E.A. Hoffman, 2009, Multiscale simulation of gas flow in subject-specific models of the human lung, IEEE Engineering in Medicine and Biology Magazine 28(3), pp. 25–33.
[11] Fluent Inc. User's Guide, 2006, 10 Cavendish Court, Lebanon, NH03766.
[12] Hofmann W, Martonen TB, Graham RC. Predicted deposition of nonhygroscopic aerosols in the human lung as a function of subject age. J Aerosol Med 1989; 2:49–68.
[13] Agustí, A. G. N. 1995, Función pulmonar aplicada: puntos clave. Mosby/Doyma Libros, Barcelona.